Dispersive determinations of lattice HVP window quantities for muon g-2

Kim Maltman, York University (and CSSM, Adelaide)

with G. Benton, D. Boito, M. Golterman, A. Keshavarzi, S. Peris

DB, MG, KM, SP, PRD107 (2023) 034512 [2210.13677 [hep-ph]]

DB, MG, KM, SP, PRD105 (2022) 093003 [2203.05070 [hep-ph]]

DB, MG, KM, SP, PRD107 (2023) 074001 [2211.11055 [hep-ph]]

GB, DB, MG, AK, KM, SP, PRL131 (2023) 251803 [2306.16808 [hep-ph]]

GB, DB, MG, AK, KM, SP, PRD109 (2024) 036010 [2311.09523 [hep-ph]]

GB, DB, MG, AK, KM, SP, in preparation (re SD, LD windows)

CONTEXT: DISPERSIVE-EXPT a_μ AND LATTICE-DISPERSIVE a_μ^{HVP} DISCREPANCIES

SM expectations for a_μ with dispersive vs lattice HVP

With new BMW 2407.10913 lattice update

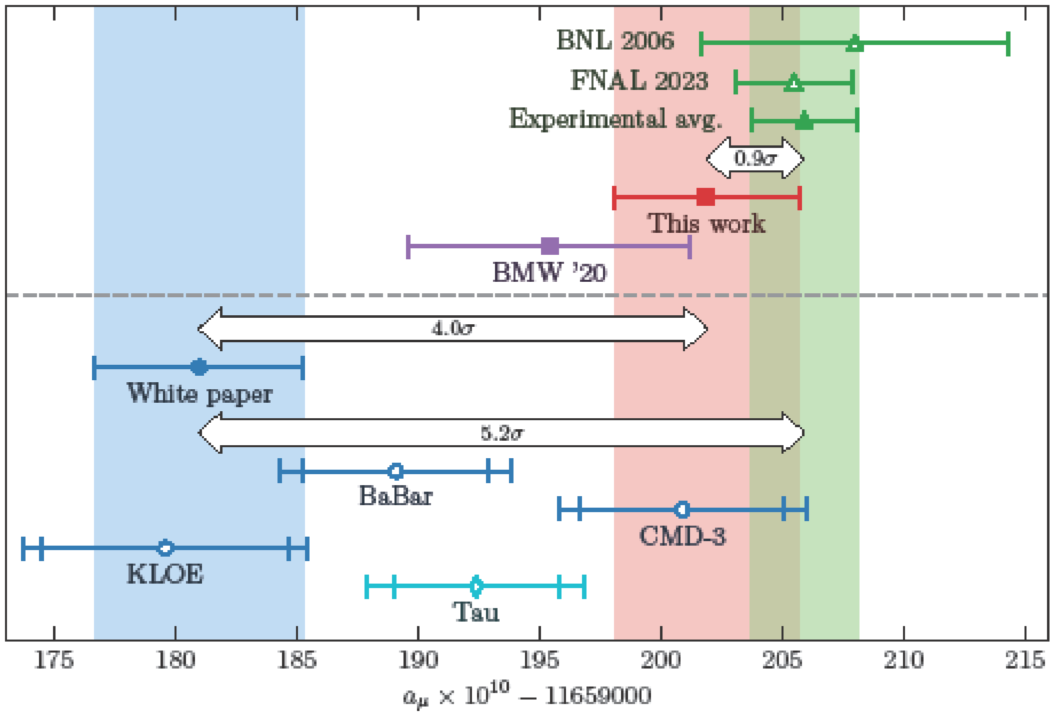

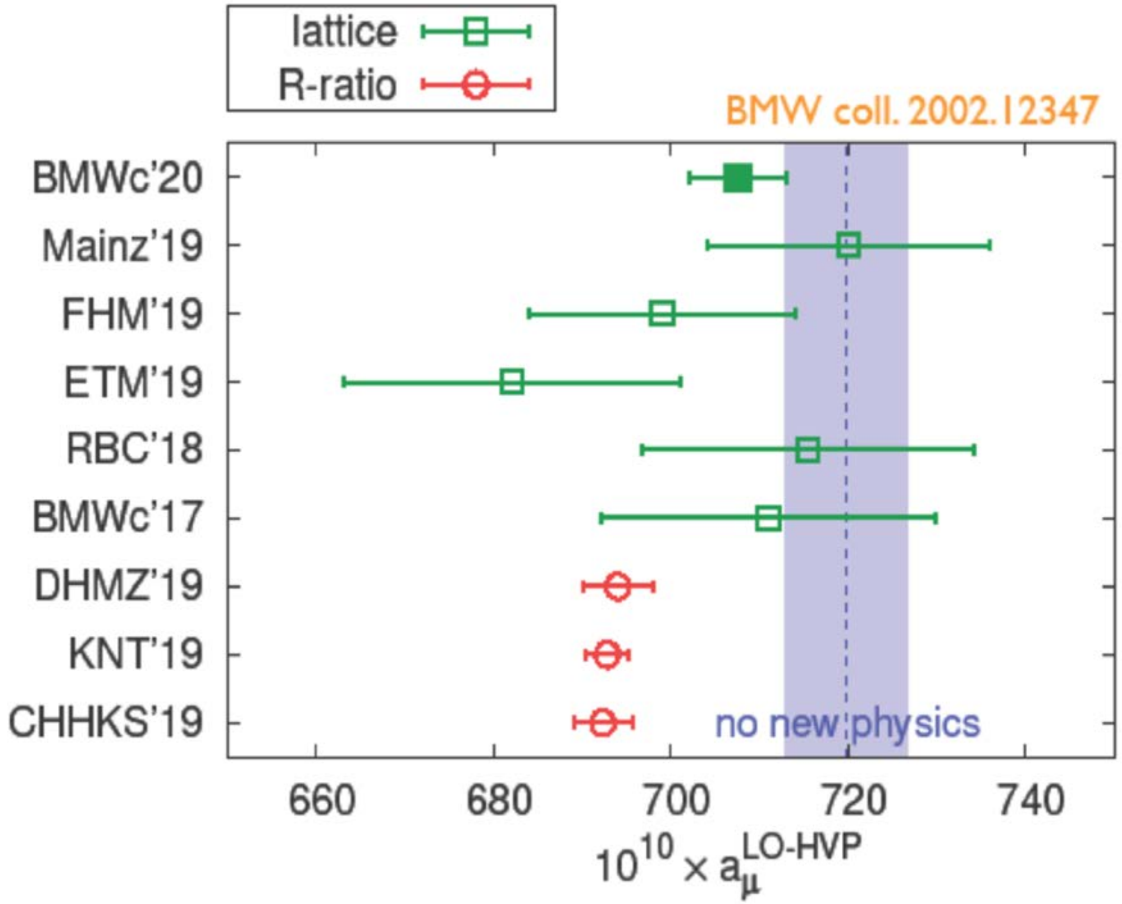

CONTEXT (2): RBC/UKQCD intermediate window (W1) HVP quantities

(post new BMW 2407.10913 lattice update)

- **IL, lqc intermediate window $a_\mu^{W1,lqc}$**

BBGKMP23: PRL 131 (2023) 251803

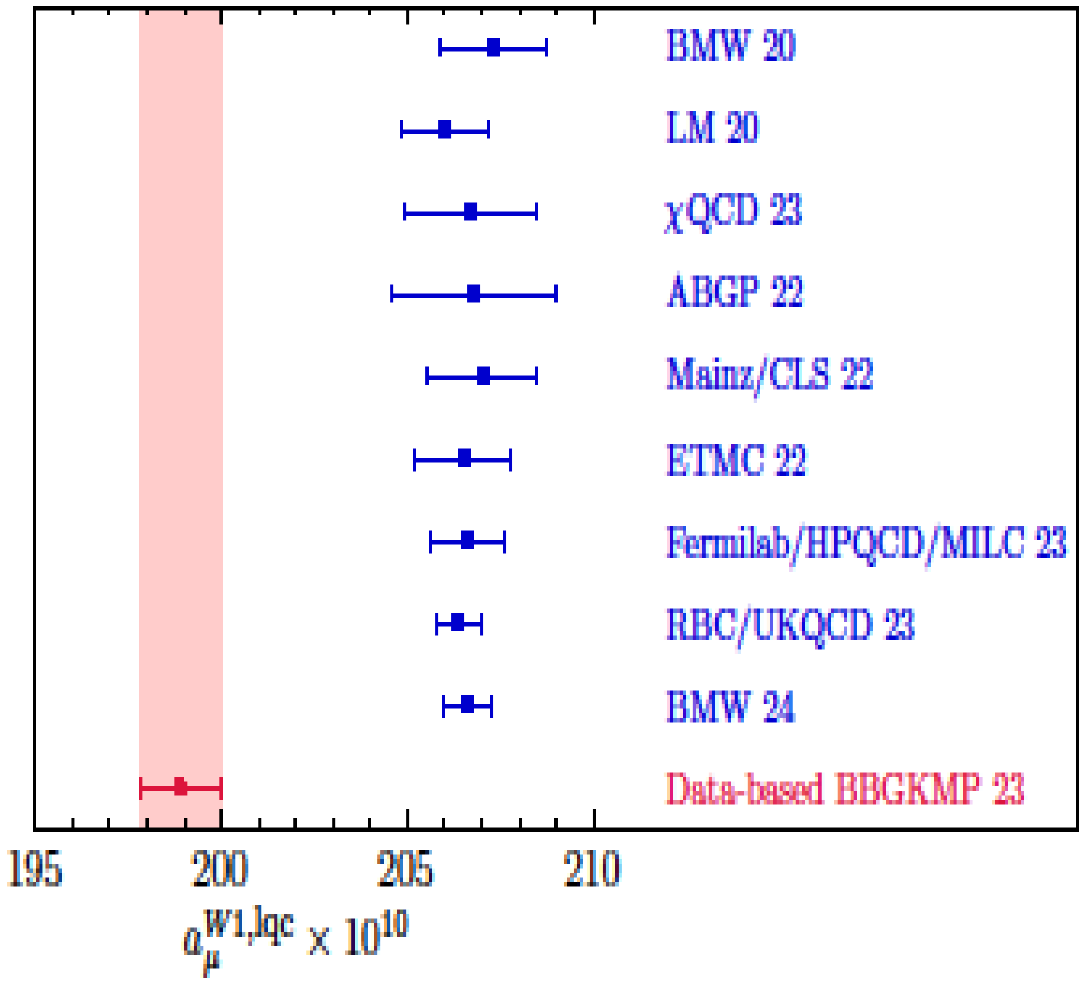

- **Full intermediate window a_μ^{W1}**

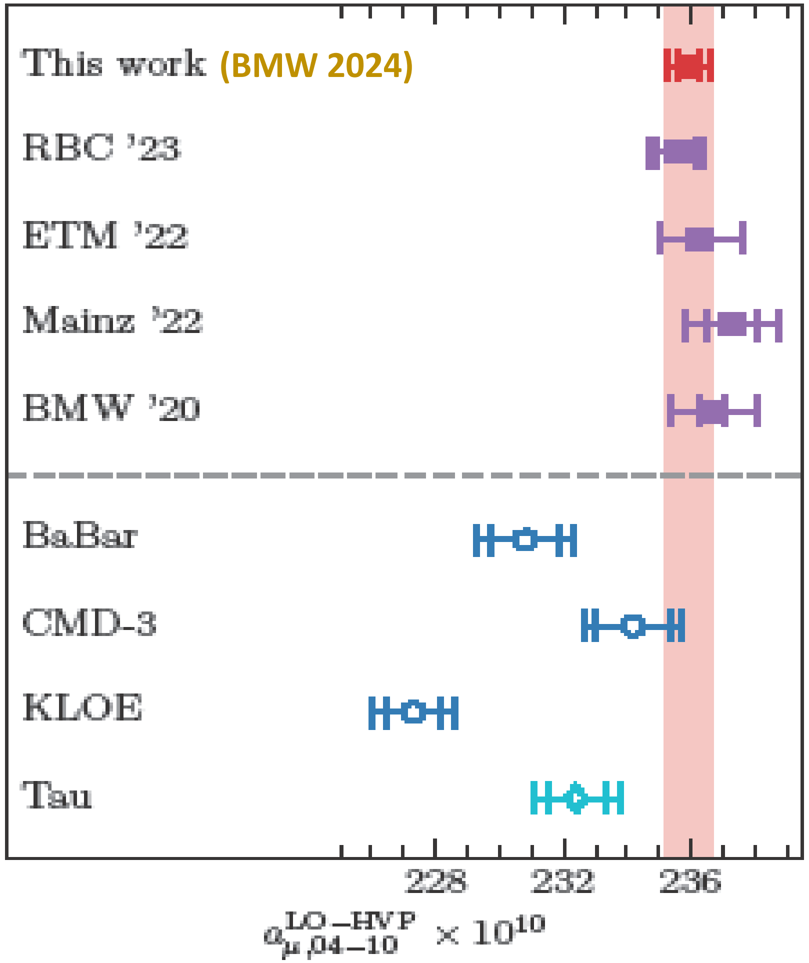

DISPERSIVE (SPECTRAL) AND LATTICE (TIME-MOMENTUM) a_μ^{HVP} REPRESENTATIONS

- **Dispersive (timelike s=q^2 spectral integral) representation:**
  - ❖ $\hat{\Pi}(Q^2)$: Q^2=0 subtracted scalar polarization of EM current-current 2-point function
  - ❖ EM spectral function $\rho(s)$ = Im $\hat{\Pi}$(-s)/π, related to R-ratio by R(s) = $12\pi^2\rho(s)$

$$a_\mu^{HVP} = \frac{4\alpha^2 m_\mu{}^2}{3} \int_{th}^{\infty} ds \, \frac{\hat{K}(s)}{s^2} \, \rho(s)$$

$\hat{K}$(s) known, monotically Increasing from ~0.63 at 2π threshold to 1 as s→∞

- **Lattice time-momentum (Euclidean time) integral representation:**

$$C(t) = \frac{1}{3}\sum_{i=1}^{3}\int d^3x \langle j_i^{\rm EM}(\vec{x},t) j_i^{\rm EM}(0)\rangle = \frac{1}{2}\int_{m_\pi^2}^{\infty} ds\,\sqrt{s}\,e^{-\sqrt{s}t}\,\rho_{\rm EM}(s) \quad (t>0)$$

Bernecker and Meyer '11

Leading order contribution to $a_\mu^{\rm HVP}$

$$a_\mu^{\rm HVP} = 2\int_0^{\infty} dt\, w(t) C(t)$$

$$\frac{\hat{K}(s)}{s^2} = \frac{3\sqrt{s}}{4\alpha^2 m_\mu^2}\int_0^{\infty} dt\, w(t)\, e^{-\sqrt{s}t}$$

LATTICE-MOTIVATED INTERMEDIATE WINDOW QUANTITIES

- **RBC/UKQCD-style intermediate window: reduce lattice errors by cutting out short- and long-t contributions**

$$a_\mu^W = 2\int_0^\infty dt\, f_W(t;\, t_0,\, t_1,\, \Delta)\, [w(t)C(t)] \qquad f_W(t;\, t_0,\, t_1,\, \Delta)) = \frac{1}{2}\left[tanh\left(\frac{t-t_0}{\Delta}\right) - tanh\left(\frac{t-t_1}{\Delta}\right)\right]$$

RBC/UKQCD (W1): ($t_{0,}$ $t_{1,}$ Δ)=(0.4, 1.0, 0.15) fm, ABGP (W2): ($t_{0,}$ $t_{1,}$ Δ)=(1.5, 1.9, 0.15) fm

- Associated short-distance (SD) and long-distance (LD) windows, with

$$f_W(t) \rightarrow f_{SD}(\mathrm{t}) = \frac{1}{2}(1 - tanh\left[\frac{t-t_0}{\Delta}\right]) \qquad f_{LD}(\mathrm{t}) = \frac{1}{2}\left(1 + tanh\left[\frac{t-t_1}{\Delta}\right]\right)$$

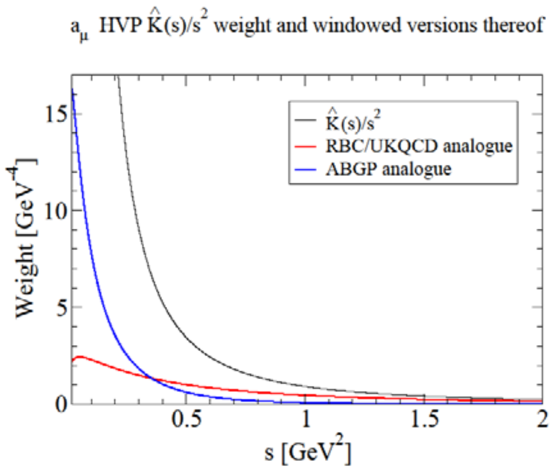

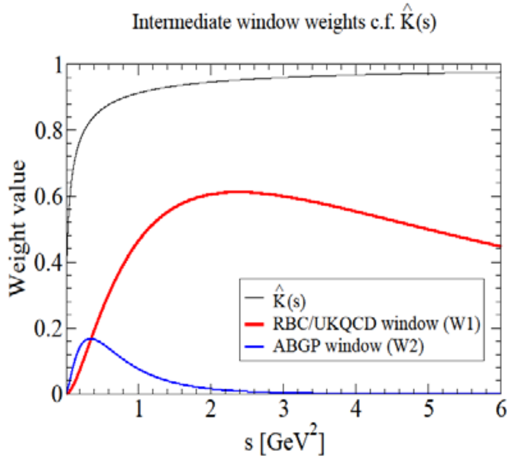

EXPONENTIAL-WEIGHT-SUM-RULE "WINDOW" QUANTITIES

- **EWSR "tuned" s-dependent-weight integral quantities** [variation on Hansen, Lupo, Tantalo PRD99 (2019) 094508]
  - Choose $\{t_k\}$, tune $\{b_k\}$ to produce s-dependent weight with ~ desired shape and form $w(s,\{t_k\}) = \frac{1}{2}\sum_k b_k \sqrt{s}\, exp(\sqrt{s}\, t_k)$ (e.g., $\widehat{W}_{15}(s)$, $\widehat{W}_{25}(s)$ below)

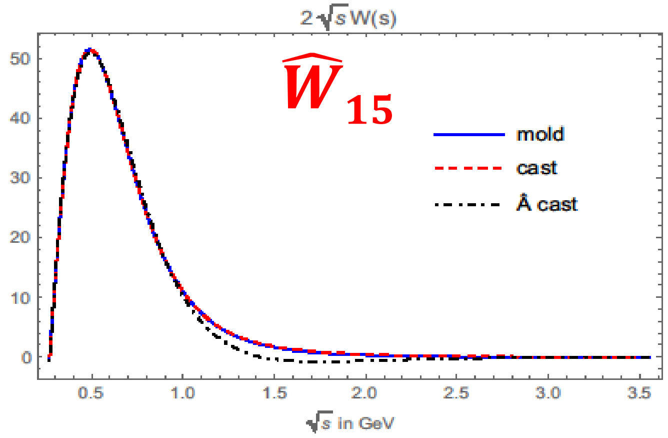

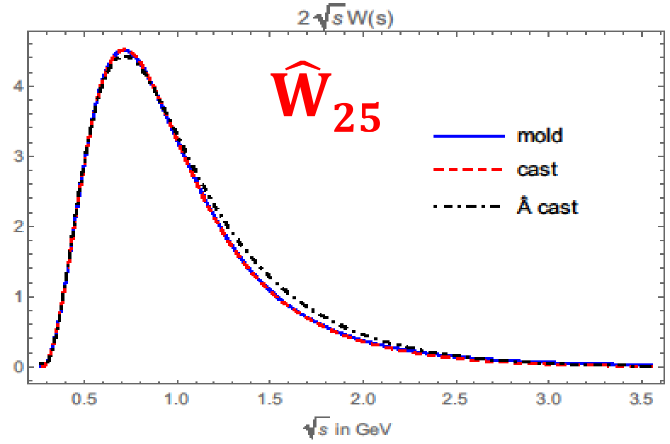

  - $\Rightarrow$ EWSR $\int_{th}^{\infty} ds\, w(s;\{t_k\})\, \rho_{EM}(s) = \sum_k b_k C(t_k)$ with tuned weight profile (in examples shown, to suppress low-s region and emphasize ρ region)
  - Restrict $\{t_k\}$ by hand to avoid large t and control lattice errors

$SU(3)_F$ decompositions

$$J_\mu^{EM} = V_\mu^3 + \frac{1}{\sqrt{3}} V_\mu^8 \equiv J_\mu^{EM,3} + J_\mu^{EM,8} + \cdots$$
$$= \frac{1}{2}\left(\bar{u}\gamma_\mu u - \bar{d}\gamma_\mu d\right) + \frac{1}{6}\left(\bar{u}\gamma_\mu u + \bar{d}\gamma_\mu d - 2\bar{s}\gamma_\mu s\right) + \cdots$$

I=1, G-parity + I=0, G-parity -

$$\hat{\Pi}_{EM}(Q^2) = \hat{\Pi}_{EM}^{33}(Q^2) + \frac{2}{\sqrt{3}}\hat{\Pi}_{EM}^{38}(Q^2) + \frac{1}{3}\hat{\Pi}_{EM}^{88}(Q^2)$$
$$= \hat{\Pi}_{EM}^{I=1}(Q^2) + \hat{\Pi}_{EM}^{MI}(Q^2) + \hat{\Pi}_{EM}^{I=0}(Q^2)$$

+ *similarly for* $\rho_{EM}(s)$, C(t)

⇒ **inherited decompositions of inclusive, exclusive-mode HVP contributions a_μ^X**

$$a_\mu^X = a_\mu^{X,33} + \frac{2}{\sqrt{3}} a_\mu^{X,38} + \frac{1}{3} a_\mu^{X,88} \equiv a_\mu^{X,I=1} + a_\mu^{X,MI} + a_\mu^{X,I=0}$$

(and analogous windowed/alternately weighted spectral integral quantities)

Isospin & quark connectedness: the "lqc" and "s+lqd" combinations

In the isospin limit: $\frac{1}{4}\langle(\bar{u}\gamma_\mu u - \bar{d}\gamma_\mu d)(x)(\bar{u}\gamma_\mu u - \bar{d}\gamma_\mu d)(y)\rangle = \frac{1}{2} x$ 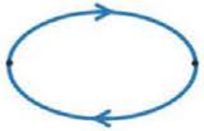 y — u, d I=1

and $\frac{1}{36}\langle(\bar{u}\gamma_\mu u + \bar{d}\gamma_\mu d)(x)(\bar{u}\gamma_\mu u + \bar{d}\gamma_\mu d)(y)\rangle = \frac{1}{18} x$ 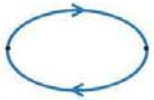 $y + \frac{1}{9} x$  y — u, d I=0

Therefore $R_{\rm EM}^{\rm sconn+disc} = R^{I=0} - \frac{1}{9} R^{I=1} \quad \to \quad R_{\rm EM}^{\rm lqc} = \frac{10}{9} R^{I=1}$

$$\Rightarrow a_\mu^{W,{\rm sconn+disc}} = a_\mu^{W,I=0} - \frac{1}{9} a_\mu^{W,I=1} \quad \to \quad a_\mu^{W,{\rm lqc}} = \frac{10}{9} a_\mu^{W,I=1}$$

s+lqd: strange connected+uds disconnected

lqc: light-quark connected

Light-flavor contributions measured on the lattice

- isospin limit (IL) light-quark (u, d) connected (lqc): **in both I=0 and 1**
- IL strange-quark connected (sconn) + uds disconnected (disc) (s+lqd) sum: **I=0 only**
- EM (connected and disconnected): **in all of I=0, I=1 and MI**
- strong isospin-breaking (SIB) (connected & disconnected): **to $O(m_d - m_u)$: MI only**
- **Ideally: evaluate all dispersively to isolate lattice-dispersive discrepancy source(s)**

DISPERSIVE STRATEGY/INPUT FOR COMPARISONS TO LATTICE

- **IL I=0/1 separation required to identify IL lqc and s+lqd contributions**
  - Separation for modes containing narrow G-parity eigenstates (π, η, ω, φ) only: I=1 for G = +, I=0 for G = - (up to IB corrections)
  - Residual G-parity mixed ("ambiguous") modes:
    - $K\bar{K}$ I=1 part of I=0+1 EM total from BaBar 2018 $\tau^- \to K^- K^0 \nu_\tau$ via CVC
    - I=0/1 $K\bar{K}\pi$ separation from BaBar 2007 Dalitz plot analysis
    - $\pi^0\gamma$, $\eta\gamma$ I=0/MI/I=1 decomposition from resonance saturation and known V=ω, φ, ρ EM decay constants, masses, widths and $V \to \pi^0\gamma$, $\eta\gamma$ widths
    - remaining exclusive-mode: "maximally conservative" $50 \pm 50\%$ $I = 1$, $50 \mp 50\%$ $I = 0$ splits
  - s-dependent exclusive-mode input from KNT19 to E_{CM}=1.937 GeV; pQCD (+DVs) for inclusive-region, E_{CM}>1.937 GeV, contributions

- **IB corrections to G-parity-classified nominally I=1/0 contributions:**
  - remove MI "contaminations" of nominally G=+/- unambiguous-mode contributions
    - Dominant: ρ-ω-induced MI contaminations of nominally I=1/I=0 2π/3π contributions: Hoferichter et al. dispersive determinations [JHEP 10(2022) 032 (CHKS22); JHEP 08(2023) 08 (HHKS23)); PRL131 (2023) 161905 (HCHKd23) for RBC/UKQCD windows, private communication for EWSR "windows"]
    - other nominally I=0, 1 modes: O(1%) additional uncertainty estimate
  - remove IB EM flavor 33, 88 contributions (unlike MI corrections, only inclusive sums needed: use lattice)

RESULTS (1): THE DISPERSIVE $a_\mu^{IL,lqc}$ DETERMINATION

[including small updates of PRD107 (2023) 074001]

- **With KNT19 input:**

$$a_\mu^{lqc,IL} = \left(\frac{10}{9}\right)\Big(543.5(2.1) + 2.9(1.0) + 28.27(2) + 0.26(12)\Big) + 1.57(55) - 4.21(47)$$

G-par +	G-par ambig	pQCD	DVs	EM IB	MI IB
95%	0.46%	5.0%		0.25%	-0.64%
				BMW 2024	CHKS22, HCHKd23

- **Full $a_\mu^{IL,lqc} \times 10^{10}$ results:**

$a_\mu^{IL,lqc} = 635.8(2.6)$ (KNT19)

$a_\mu^{IL,lqc} = 638.9(4.1)$ (DHMZ)

c.f. lattice: C. Lehner Lattice2024

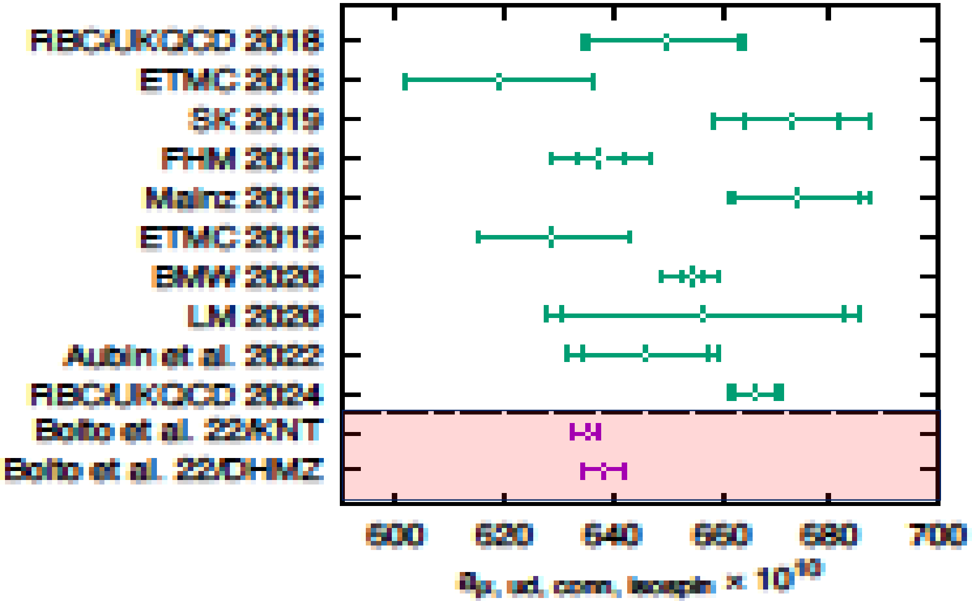

- **Tension w/ lattice (BMW20, RBCUKQCD24)**

RESULTS (2): RBC/UKQCD INTERMEDIATE WINDOW lqc [$a_\mu^{W1,lqc}$] RESULTS

G=+ mode X	$a_{\mu,X}^{W1}$ x 10^{10}
low-s $\pi^+\pi^-$	0.02(00)
$\pi^+\pi^-$	144.13(49)
$2\pi^+2\pi^-$	9.29(13)
$\pi^+\pi^-2\pi^0$	11.94(48)
$3\pi^+3\pi^-$ (no ω)	0.14(01)
$2\pi^+2\pi^-2\pi^0$ (no η)	0.83(11)
$\pi^+\pi^-4\pi^0$ (no η)	0.13(13)
$\eta\pi^+\pi^-$	0.85(03)
$\eta 2\pi^+2\pi^-$	0.05(01)
$\eta\pi^+\pi^-2\pi^0$	0.07(01)
$\omega(\to\pi^0\gamma)\pi^0$	0.53(01)
$\omega(\to$ npp$)3\pi$	0.10(02)
$\omega\eta\pi^0$	0.15(03)
TOTAL	168.24(72)

$a_\mu^{W1,lqc}$ contributions (in units of 10^{10})

- G=+: 186.93(80)
- $K\bar{K}$: 0.58(7)
- $K\bar{K}\pi$: 0.52(9)
- $K\bar{K}\pi\pi$: 0.60(60)
- $\pi^0\gamma$ 0.07(1)
- $\eta\gamma$ 0.06(0)
- other mixed G: 0.05(5)
- pQCD$\pm DVs$: 11.06$\pm$0.16
- EM corr'n: -0.04(6)
- 2π ($\pm$other) MI corr'n: -0.92(7)$\pm$0.29

$a_\mu^{W1,lqc}$ = 198.9(1.1) x 10^{-10}

G. Benton, PRL131 (2023) 251803, updated

RESULTS (2'): DISPERSIVE-LATTICE $a_\mu^{W1,lqc}$ COMPARISON

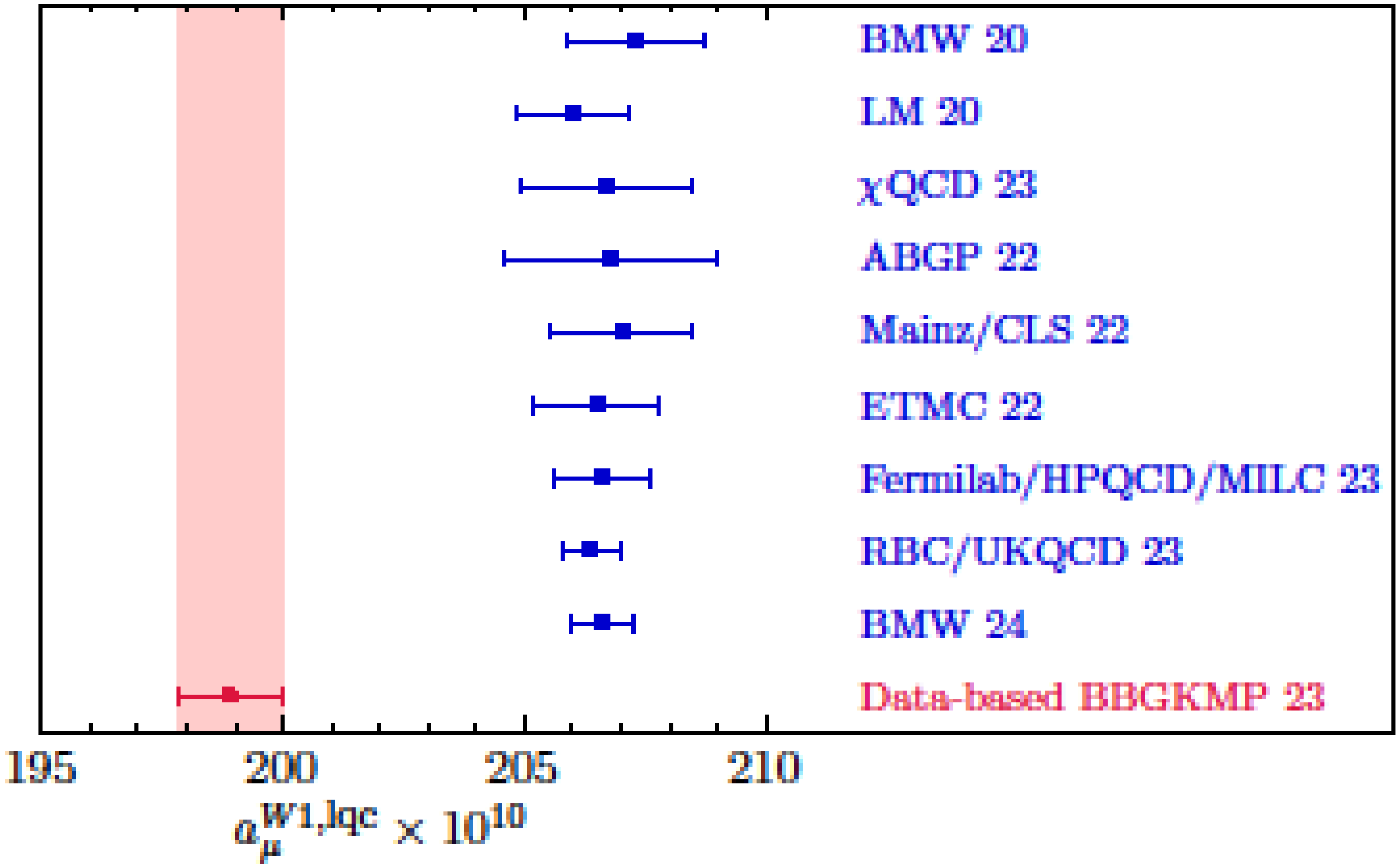

Large dispersive-lattice W1 IL, lqc discrepancy (e.g., 6σ for latest BMW 2024)

RESULTS (3): DISPERSIVE vs LATTICE IL, s+lqd AND OTHER-WINDOW IL, lqc

- Lattice EM results not available for other intermediate windows so neglect EM I=0, 1 corrections for now (plausible based on W1 result)
- For RBC/UKQCD SD window EM: O(α_{EM}*SD) or Mainz 2024 0.15(15)% SD_{EM}/SD result estimates
- RBC/UKQCD LD window: $LD_{EM} = HVP_{EM} – W1_{EM} - SD_{EM}$
- For IL, lqc cases, windowed versions of CHKS22 2π MI correction (from M. Hoferichter and P. Stoffer: thanks!)
- IL, s+lqd cases need also windowed ρ-ω region 3π MI correction of HHKS23 (provided by the authors: thanks!)
- **Compare IL dispersive and lattice results where latter available**

ABGP22 INTERMEDIATE WINDOW (W2) RESULTS

- **RBC/UKQCD-style intermediate window, designed to be longer distance, more amenable to possible use of ChPT for FV** [Aubin et al. PRD106 (2022) 054503]

light-quark connected from KNT19 R(s) data

$$a_\mu^{W2,\mathrm{lqc}} = 93.70(36) \times 10^{-10}$$

Benton, et al. PRD109 (2024) 036010

Includes -0.85(4) x 10^{-10} MI IB correction

lattice results

Aubin, Blum, Golterman, Peris '22

$$a_\mu^{W2,\mathrm{lqc}} = 102.1(2.4) \times 10^{-10}$$

Fermilab/HPQCD/MILC '23

$$a_\mu^{W2,\mathrm{lqc}} = 100.7(3.2) \times 10^{-10}$$

BMW 2407.10813

$$a_\mu^{W2,lqc} = 97.67(1.62) \times 10^{-10}$$

ABGP update soon (see V. Moningi, Lattice2024)

EWSR WEIGHT ($\widehat{W}_{15}$, $\widehat{W}_{25}$) IL, lqc RESULTS

- $I_W^{lqc} \equiv \int_{th}^{\infty} ds\, \mathrm{W(s)}\, \rho_{EM}^{IL,lqc}(\mathrm{s})$

lqc from KNT19 R(s) data

$$I^{\mathrm{lqc}}_{\widehat{W}_{15}} = 42.78(16) \times 10^{-2}$$

$$I^{\mathrm{lqc}}_{\widehat{W}_{25}} = 78.85(46) \times 10^{-3}$$

Benton, et al. PRD109 (2024) 036010

5.6σ

3.2σ

ABGP lqc lattice data

$$I^{\mathrm{lqc}}_{\hat{W}_{15}} = 46.69(68) \times 10^{-2}$$

$$I^{\mathrm{lqc}}_{\hat{W}_{25}} = 82.4(1.0) \times 10^{-3}$$

systematic errors on lattice results still to be assessed

IB correction contributions:

$\widehat{W}_{15}$: -0.37 x 10^{-2}

$\widehat{W}_{25}$: -0.33 x 10^{-3}

- **Another sign of dispersive-lattice IL, lqc ρ-region tension**

IL s+lqd HVP RESULTS

- **Update of PRD105 (2022) 093003 (final CHKS22 MI 2π, new HHKS23 MI 3π corrections)**
  - With KNT19 exclusive-mode contributions [Benton et al., PRD109(2024) 036010]

$$a_\mu^{s+lqd}\text{x}10^{10} = -5.26(99) + 35.12(31) + 1.89(18) + 0.95(98) + 0.10(8)$$

G-par unambig $\quad K\bar{K} \quad K\bar{K}\pi \quad K\bar{K}\pi\pi \quad$ other G-par ambig

$$+ 6.28(25) - 0.04(13) - [-2.68(99) - (1/9)\,3.79(19) \pm 0.4] = 41.4(1.5)$$

pQCD±DVs $\quad$ I=0,1 EM $\quad$ MI 3π $\quad$ MI 2π $\quad$ other MI

  - With, instead, DHMZ exclusive-mode contributions: $a_\mu^{s+lqd}\text{x}10^{10} = 39.8(2.0)$
  - No sign of discrepancy with lattice: RBC/UKQCD: 42.0(4.0); BMW (2017): 40.9(2.1); Mainz 2019 sconn+prelim 2020 disc: 39.7(3.7); BMW 2020: 40.0(1.8)
- **Similarly, for $a_\mu^{W1,s+lqd}$ x 10^{10} = 27.0(8)** [PRD109(2024) 036010] **c.f. 26.0(6) BMW2020/24**

PRELIMINARY DISPERSIVE RBC/UKQCD IL SD, LD WINDOW lqc RESULTS

- Benton et al. 2024 (preliminary): with (i) SD EM $\simeq 0 \pm (\alpha_{EM}$*SD) or using Mainz 2024 0.15(15)% relative size assessment; (ii) LD EM = $[\text{HVP EM} - \text{W1 EM}]_{BMW20/24}$-SD EM
- $a_\mu^{SD} \text{x} 10^{10} = 46.96(54)/46.89(42)$
  - ➢ **ETM22: PRD107 (2023) 074506**
  - ➢ **RBC/UKQCD23: PRD108 (2023) 054507**
  - ➢ **Mainz24: JHEP03 (2024) 172**
  - ➢ **BMW24: arXiv:2407.10913**
  - ➢ **RBC/UKQCD24: Spiegel Lattice2024**
  - ➢ **Dispersive: Benton et al. 2024**

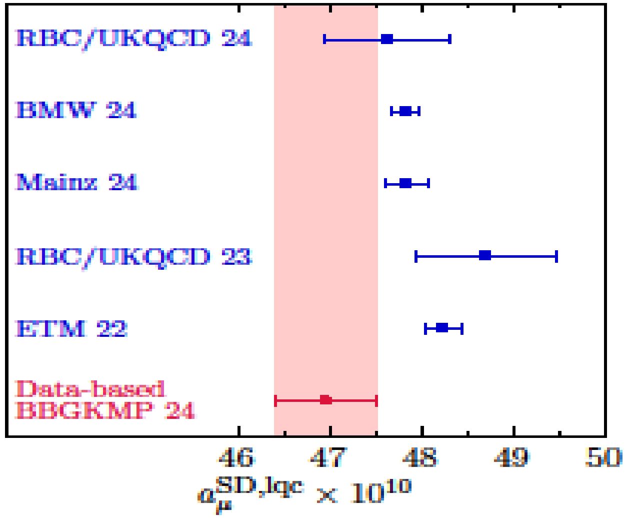

- $a_\mu^{LD} \text{x} 10^{10}$ =389.9(1.7)/390.0(1.7)
  - ➢ **RBC/UKQCD24: C. Lehner Lattice 2024**
  - ➢ **Dispersive: Benton et al. 2024**

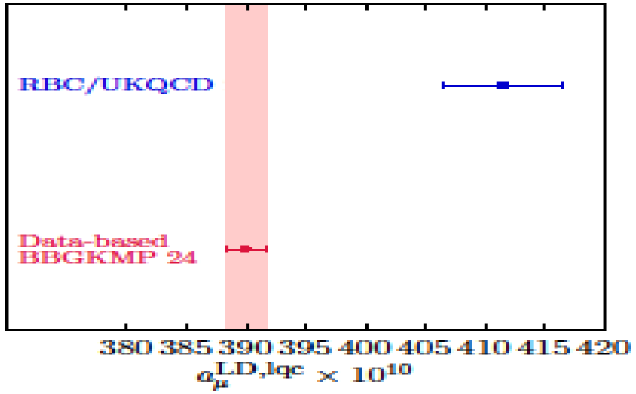

- **SD, LD IL s+lqd results also coming**

INTERIM CONCLUSIONS

- With current EM R(s) data, further evidence for a significant dispersive-lattice discrepancy, especially for IL, lqc RBC/UKQCD intermediate window (W1) and improved EWSR $\widehat{W}_{15}$ weighting
- Pattern of discrepancies points to source in dispersive ρ region contributions
- C(t) results needed to determine a_μ^{HVP} and a_μ^{W1} and/or components thereof also provide results for SD, LD windows and the lattice side of any related EWSR: further exploration of EWSR weight choices in conjunction with new lattice data thus also of interest
- **An obvious question still to be dealt with: the impact on the lattice-dispersive discrepancies of the new CMD-3 ππ data [PRD109(2024) 112002 [2302.08834]]?**

Impact of 2023 CMD-3 ππ results on $a_\mu^{W1,lqc}$ and a_μ^{HVP}

- NOTE: Exploration only, replacing all other ππ data in CMD-3 region with CMD-3

$a_\mu^{W1,lqc}$

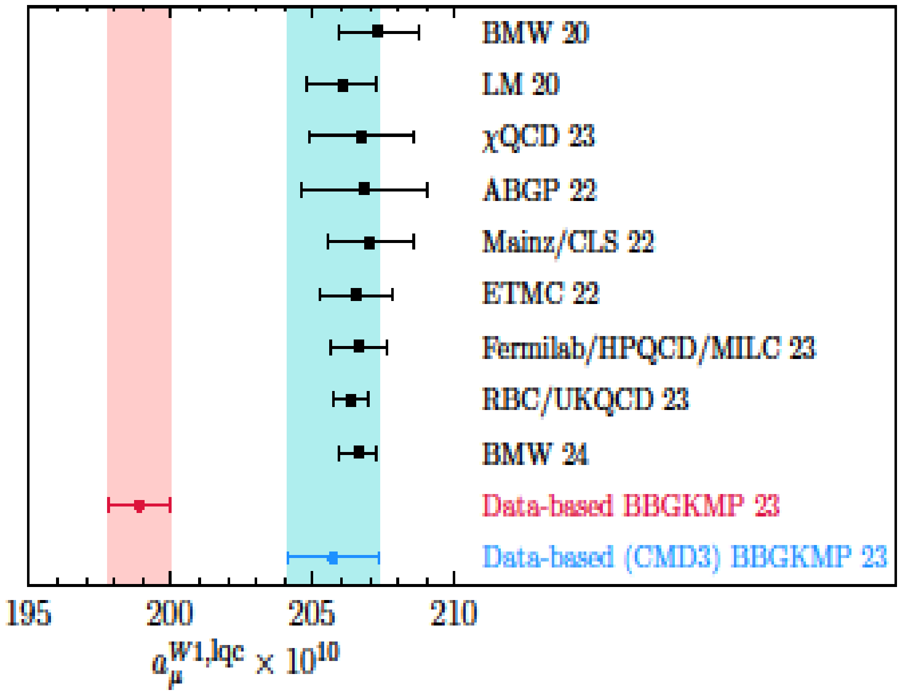

With CMD-3: 205.6(1.6) x 10^{-10}

a_μ^{HVP} (including BMW24 hybrid)

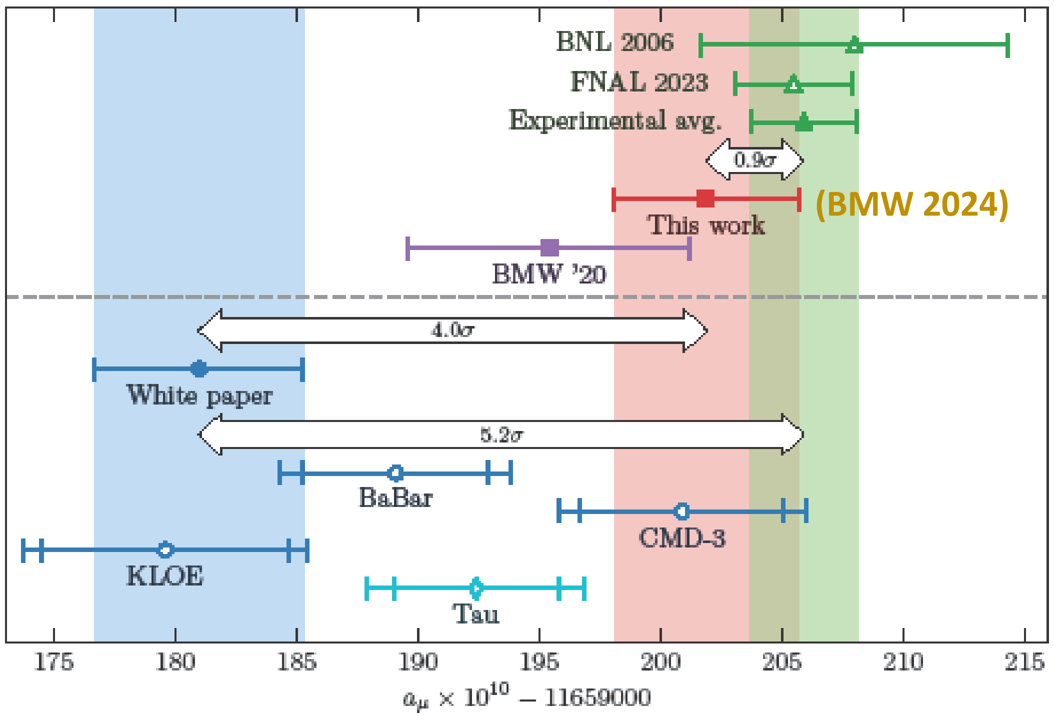

Impact on IL, lqc W2, RBC/UKQCD SD, LD, and $\widehat{W}_{15}$ and $\widehat{W}_{25}$ results

- IL, lqc ABGP W2

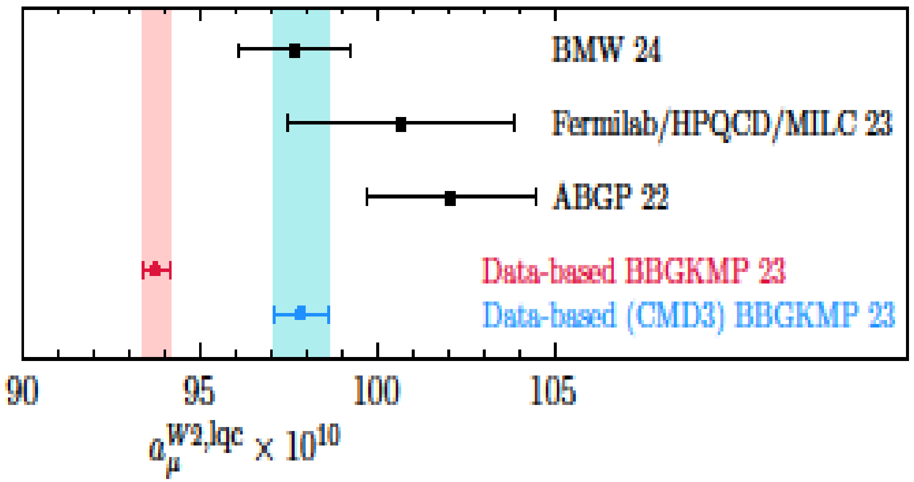

- RBC/UKQCD IL, lqc SD and LD

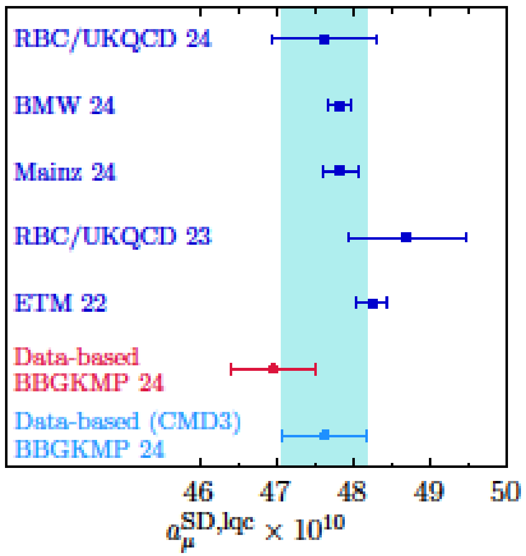

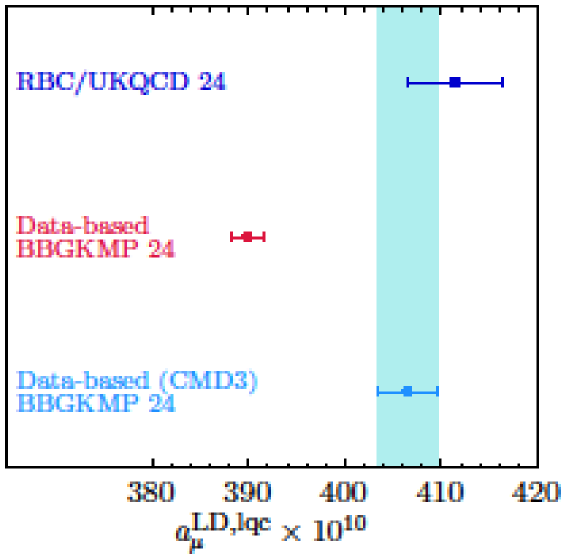

- EWSR weight discrepancies [recall, lattice errors statistical only]
  - W_{15} IL, lqc KNT19 result 0.4278(16) → $0.4483(37)$ c.f. lattice $0.4669(58)$ ($5.6\ \sigma \to 2.7\ \sigma$)
  - $\widehat{W}_{25}$ IL, lqc KNT19 result 0.0789(5) → $0.0815(6)$ c.f. lattice $0.0824(10)$ ($3.2\ \sigma \to 0.8\ \sigma$)

All dispersive-lattice differences strongly reduced with CMD-3 ππ input